Electronic Supplementary Material (ESI) for Physical Chemistry Chemical Physics.

Supporting information for

Phosphine oxides as NMR and IR spectroscopic probes for geometry and energy of PO···H–A hydrogen bonds

M.A. Kostin,[1] S.A. Pylaeva,[2] P.M. Tolstoy[3,*]

[1] Department of Physics, St.Petersburg State University, St. Petersburg, Russia

[2] Chair of Theoretical Chemistry, University of Paderborn, Paderborn, Germany

[3] Institute of Chemistry, St.Petersburg State University, St. Petersburg, Russia

* corresponding author, peter.tolstoy@spbu.ru

Optimized geometries (tight convergence criteria), energies and harmonic vibration frequencies were calculated using the same level of theory that was used for the PCM calculations, discussed in the main text (B3LYP/6-311++G(d,p)). The complexation energy ΔE was computed as the energy needed to separate interacting molecules to an infinite distance, including the relaxation energy of monomers and basis set superposition error (BSSE; accounted for by counterpoise method applied to optimized geometry) and not including the dispersion correction. The NMR shielding constants were calculated using the same approach and the same level of theory that were desctibed in main text for calculations in aprotic medium. The P=O stretching vibrational frequencies are reported relative to that in free Me_3PO molecule, $\nu_{P=O}$ = 1204.35 cm^{-1}.

Text 1. Computational details for calculations in the gas phase.

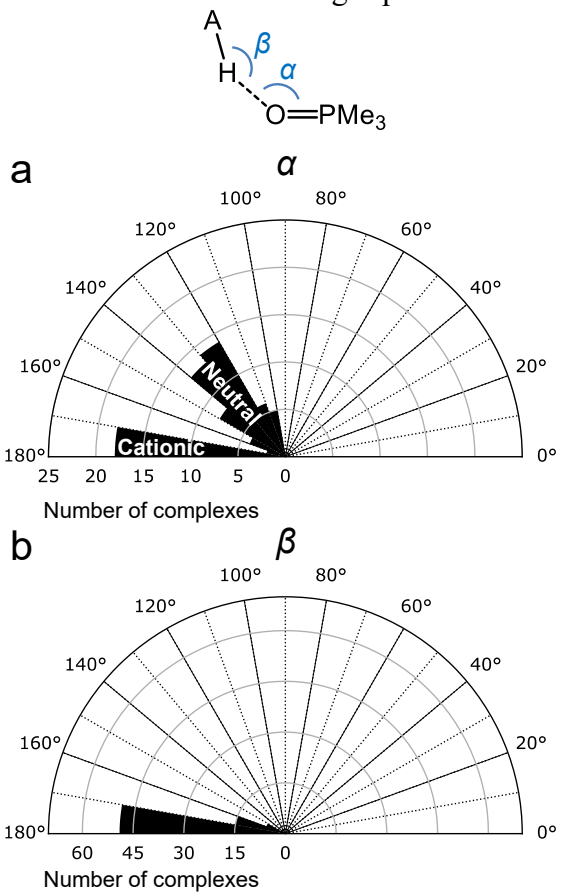

Figure S1. The complexes of Me_3PO in the gas phase: distribution diagrams of valence angles α (**a**) and β (**b**) in investigated complexes of Me_3PO with proton donor molecules.

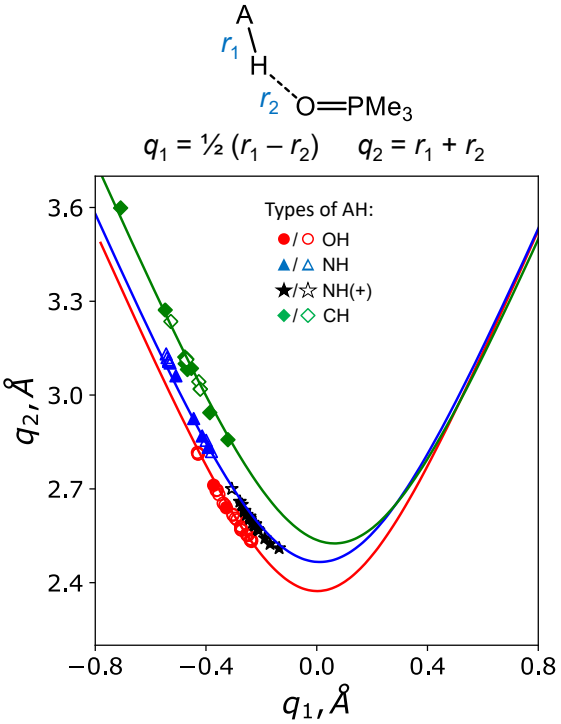

Figure S2. The complexes of Me_3PO in the gas phase: correlation between q_2 and q_1 natural coordinates of hydrogen bond in complexes. The solid lines correspond to **Eqs. 1–3**. For more details see text.

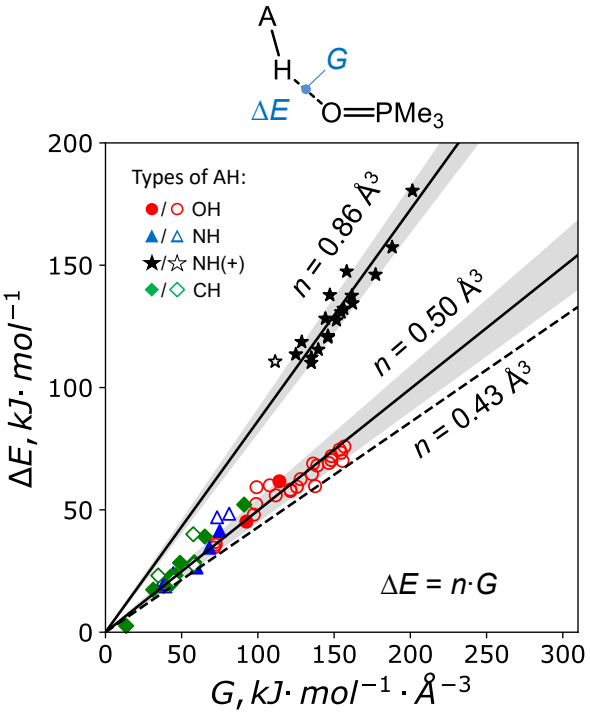

Figure S3. The complexes of Me_3PO in the gas phase: correlation between hydrogen bond energy ΔE and local electron kinetic energy density G. Solid lines correspond to equation $\Delta E = n \cdot G$. The coefficient n is different for complexes with cationic $n = (0.86 \pm 0.04)$ Å^3 and neutral AH molecules $n = (0.43 \pm 0.04)$ Å^3. Grey areas indicate the standard error of fitted n values. Dashed line ($n = 0.43$ Å^3) is built according to the literature data (M. V. Vener, A. N. Egorova, A. V. Churakov and V. G. Tsirelson, *J. Comput. Chem.*, 2012, **33**, 2303–2309; I. Mata, I. Alkorta, E. Espinosa and E. Molins, *Chem. Phys. Lett.*, 2011, **507**, 185–189).

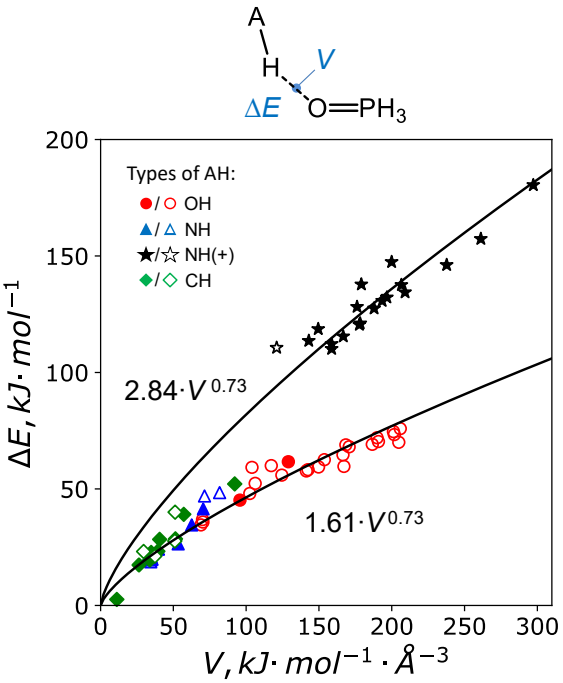

Figure S4. The complexes of Me_3PO in the gas phase: correlation between hydrogen bond energy ΔE and local electron potential energy density V. Solid lines correspond to the result of least squares fitting of data points by the functions $\Delta E = k \cdot V^{0.73}$. The coefficient k is different for complexes with cationic and neutral AH molecules. The power equal to 0.73 was fixed.

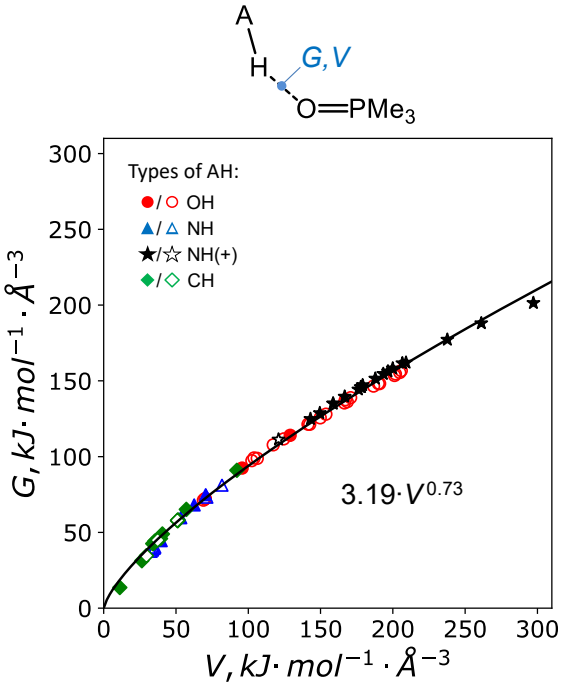

Figure S5. The complexes of Me_3PO in the gas phase: correlation between local electron kinetic energy density G and local electron potential energy density V. Solid line corresponds to the result of least squares fitting of data points by the function $G = k \cdot V^d$ for both complexes with neutral and cationic AH molecules.

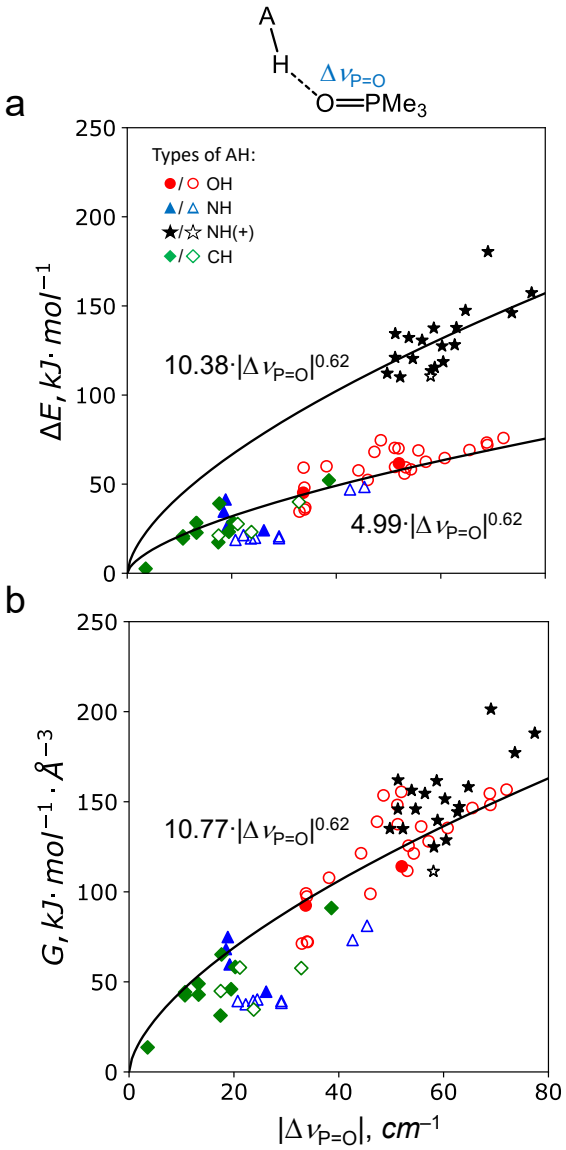

Figure S6. The complexes of Me_3PO in the gas phase: correlations $\Delta E(|\Delta\nu_{P=O}|)$ (**a**) and $G(|\Delta\nu_{P=O}|)$ (**b**). Solid lines correspond to the results of least squares fitting of data points by the power functions. The power equal to 0.62 was fixed. The correlation $\Delta E(|\Delta\nu_{P=O}|)$ is different for complexes with cationic and neutral AH molecules. The correlation $G(|\Delta\nu_{P=O}|)$ is the same for both complexes with neutral and cationic molecules.

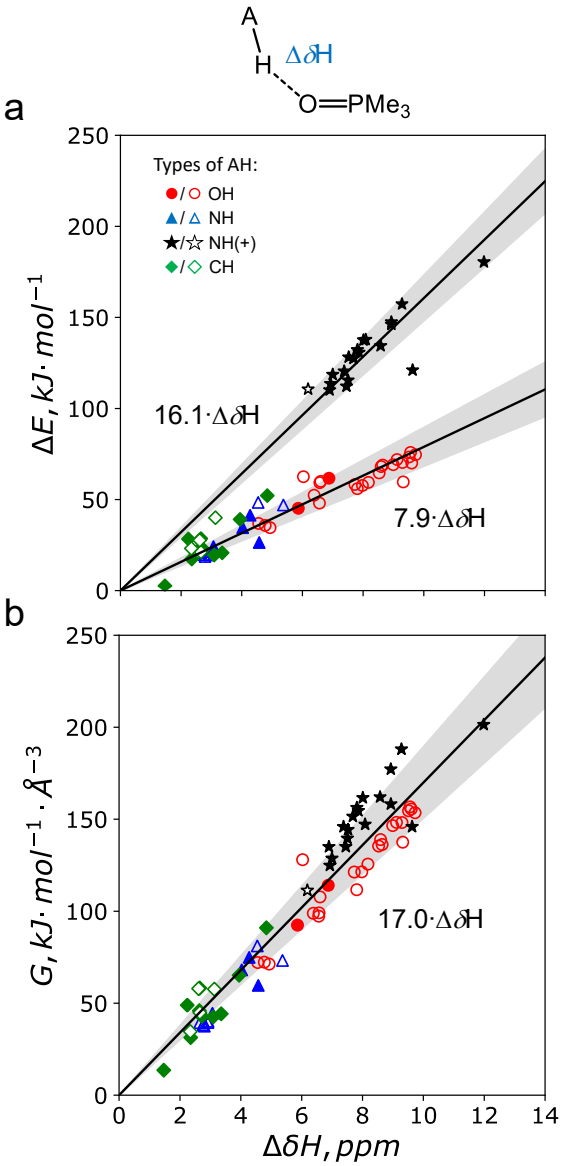

Figure S7. The complexes of Me_3PO in the gas phase: correlations $\Delta E(\Delta\delta H)$ (**a**) and $G(\Delta\delta H)$ (**b**). Solid lines correspond to the results of least squares fitting of data points by the linear functions. The correlation $\Delta E(\Delta\delta H)$ is different for complexes with cationic and neutral AH molecules. The correlation $G(\Delta\delta H)$ is the same for both complexes with neutral and cationic molecules. Grey areas indicate the standard error of fitted values.

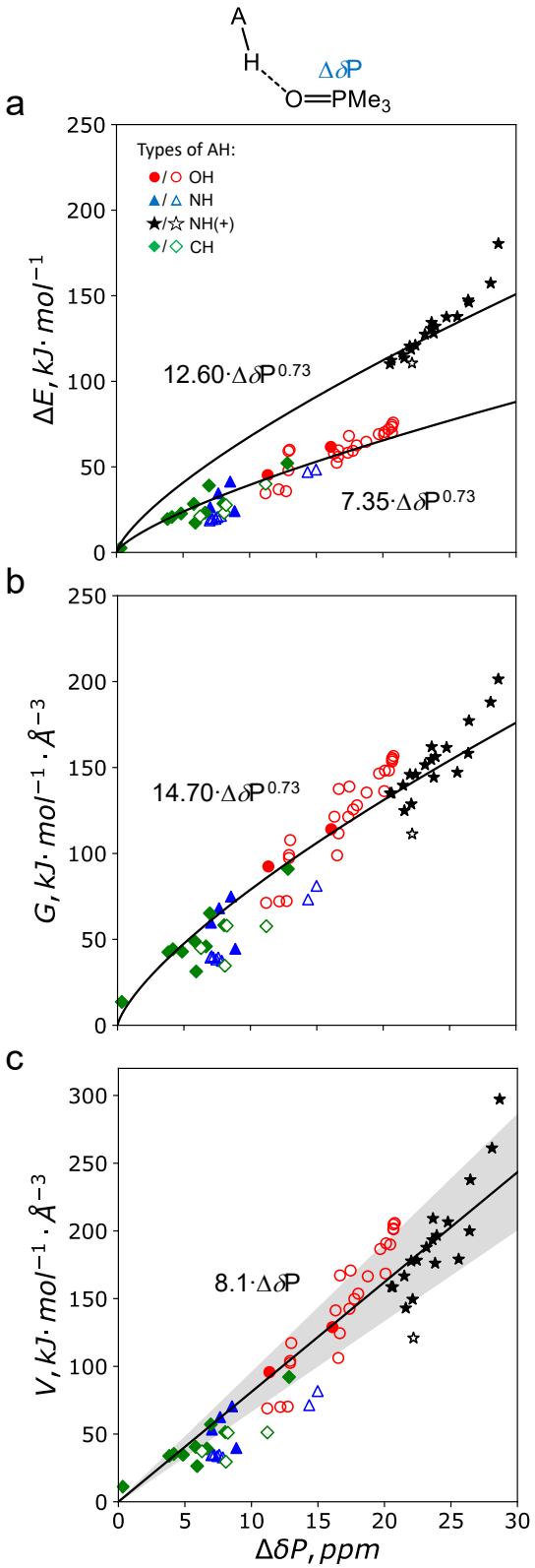

Figure S8. The complexes of Me_3PO in the gas phase: correlations between $\Delta\delta$P and hydrogen bond energy ΔE (**a**), local electron kinetic energy density G (**b**) and local electron potential energy density V (**c**). Solid lines correspond to the results of least squares fitting of data points. The correlation between V and $\Delta\delta$P is linear. The fitting of correlations $\Delta E(\Delta\delta P)$ and $G(\Delta\delta P)$ are performed by the power functions $\Delta E = a\cdot\Delta\delta P^{0.73}$ and $G = b\cdot\Delta\delta P^{0.73}$. The power equal to 0.73 was fixed due to correlation $\Delta E(G)$ (Figure S3) and $G(V)$ (Figure S5). Grey area indicates the standard error of fitted values.

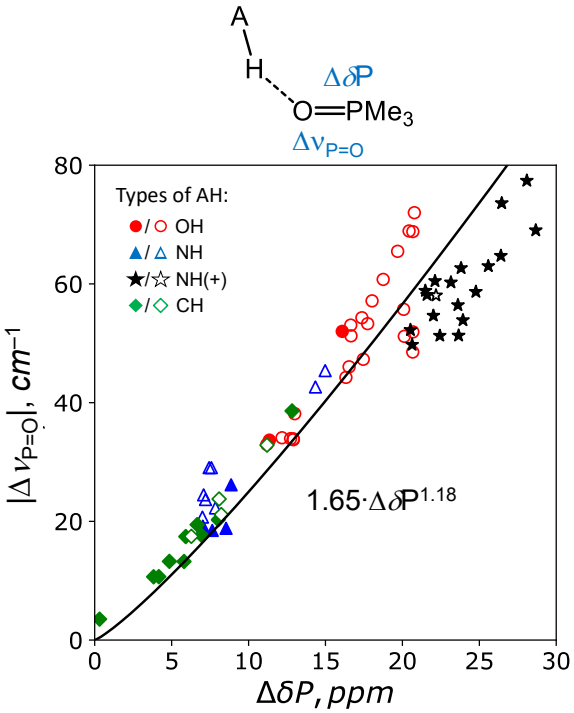

Figure S9. The complexes of Me_3PO in the gas phase: correlation between $|\Delta\nu_{P=O}|$ and $\Delta\delta P$. Solid line corresponds to the function obtained as the results of least squares fitting of correlations $G(|\Delta\nu_{P=O}|)$ shown in Figure S6 and $G(\Delta\delta P)$ shown in Figure S8. Correlation between $|\Delta\nu_{P=O}|$ and $\Delta\delta P$ is same for both complexes with cationic and neutral AH molecules.

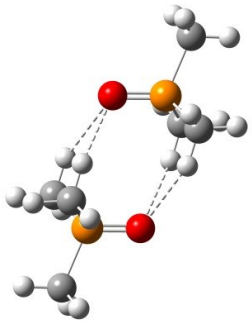

Figure S10. The structure $Me_3PO\cdots Me_3PO$ in aprotic medium (chloroform).

Table S1. Calculations at different levels of theory: geometric, energetic and spectroscopic parameters for some studied complexes in aprotic medium. Theory levels used: M062X/6–311++G(d,p), B3LYP/aug–cc–pVDZ, MP2/aug–cc–pVDZ and B3LYP/6–311++G(d,p) with Grimme's D3 dispersion correction.[a] The numerical values are given in the following units: ΔE in kJ mol^{-1}, G in kJ mol^{-1} Å^{-3}, $q_1 = 0.5\cdot(r_1 - r_2)$ and $q_2 = r_1 + r_2$ in Å, α and β in degrees, $\Delta\delta$H and $\Delta\delta$P in ppm and $\Delta\nu_{P=O}$ in cm^{-1}.

Type of proton donor	No.	Proton donor molecule	*Method/ basis set*	ΔE	G	q_1	q_2	α	β	$\Delta\delta$H	$\Delta\delta$P	$\Delta\nu$
OH	2	Methanol	B3LYP/ 6–311++G(d,p)	35.80	72.3	–0.429	2.811	110.8	160.7	4.8	12.7	33.9
			B3LYP/ 6–311++G(d,p) with GD3	34.81	69.8	–0.438	2.830	103.2	155.1	4.7	13.5	37.5
			M062X/ 6–311++G(d,p)	47.36	72.8	–0.443	2.832	102.4	149.7	4.7	13.1	40.4
			B3LYP/ aug–cc–pVDZ	35.20	69.9	–0.421	2.803	105.7	162.2	5.0	12.0	33.7
			MP2/ aug–cc–pVDZ	27.43	74.8	–0.419	2.804	100.2	158.9	4.9	12.8	34.8
	22	Phenol	B3LYP/ 6–311++G(d,p)	45.21	92.4	–0.372	2.712	130.4	172.7	5.9	11.4	33.7
			B3LYP/ 6–311++G(d,p) with GD3	36.74	91.7	–0.377	2.726	119.4	160.6	5.7	13.1	42.0
			M062X/ 6–311++G(d,p)	62.21	94.4	–0.382	2.727	118.3	157.6	5.6	13.5	48.1
			B3LYP/ aug–cc–pVDZ	44.70	91.5	–0.363	2.706	115.2	169.6	6.0	12.7	38.5
			MP2/ aug–cc–pVDZ	10.74	91.1	–0.375	2.736	110.7	155.1	5.0	12.7	45.2
	24	3–Nitrophenol	B3LYP/ 6–311++G(d,p)	59.27	99.1	–0.353	2.682	150.2	175.3	10.6	12.9	33.8
			B3LYP/ 6–311++G(d,p) with GD3	53.98	107.0	–0.339	2.663	131.4	169.1	6.9	16.0	46.7
			M062X/ 6–311++G(d,p)	75.63	104.8	–0.351	2.674	141.3	168.6	6.8	16.4	49.4
			B3LYP/ aug–cc–pVDZ	56.50	99.0	–0.343	2.671	141.1	178.7	6.6	14.5	37.0
			MP2/ aug–cc–pVDZ	35.15	115.5	–0.320	2.643	116.9	168.1	7.2	17.1	50.4

NH	**34**	Pyrrole	B3LYP/ 6–311++G(d,p)	34.58	68.1	–0.414	2.869	143.4	175.1	11.5	7.6	18.5
			B3LYP/ 6–311++G(d,p) with GD3	28.82	62.5	–0.443	2.928	112.3	151.6	3.7	11.5	33.6
			M062X/ 6–311++G(d,p)	48.39	63.2	–0.458	2.954	115.0	140.6	3.3	10.7	33.0
			B3LYP/ aug–cc–pVDZ	33.11	63.8	–0.413	2.877	121.4	170.3	4.0	9.6	26.8
			MP2/ aug–cc–pVDZ	11.86	68.5	–0.417	2.893	109.6	147.6	3.8	12.0	34.5
	35	Imidazole	B3LYP/ 6–311++G(d,p)	41.40	74.9	–0.392	2.833	149.5	176.7	12.4	8.5	18.8
			B3LYP/ 6–311++G(d,p) with GD3	34.45	72.6	–0.408	2.867	115.5	155.4	4.2	12.3	35.6
			M062X/ 6–311++G(d,p)	50.17	69.2	–0.436	2.916	117.0	141.7	3.6	11.5	34.8
			B3LYP/ aug–cc–pVDZ	39.60	71.2	–0.389	2.833	135.6	176.5	4.2	9.9	24.3
			MP2/ aug–cc–pVDZ	22.64	79.8	–0.380	2.830	107.8	157.6	4.6	13.8	38.0
	37	1,4–Dihydropyrazine	B3LYP/ 6–311++G(d,p)	26.43	59.7	–0.444	2.925	137.3	174.2	5.9	7.0	19.2
			B3LYP/ 6–311++G(d,p) with GD3	22.44	54.8	–0.473	2.983	106.1	152.9	3.9	10.1	28.6
			M062X/ 6–311++G(d,p)	39.50	51.1	–0.510	3.052	106.4	136.0	3.5	9.3	32.7
			B3LYP/ aug–cc–pVDZ	24.62	53.4	–0.454	2.953	114.2	166.5	4.1	9.2	25.0
			MP2/ aug–cc–pVDZ	8.15	63.3	–0.437	2.927	101.3	155.7	5.1	11.8	30.3
NH^+	**39**	Dimethylammonium	B3LYP/ 6–311++G(d,p)	147.44	158.2	–0.221	2.587	174.8	177.5	13.2	26.4	64.7
			B3LYP/ 6–311++G(d,p) with GD3	146.98	164.3	–0.214	2.575	171.1	173.6	9.2	26.0	60.9
			M062X/ 6–311++G(d,p)	154.23	176.5	–0.199	2.555	166.0	168.2	10.0	27.5	72.8
			B3LYP/ aug–cc–pVDZ	144.02	159.0	–0.220	2.591	161.2	171.6	8.8	24.8	64.1

			MP2/ aug–cc–pVDZ	134.40	203.7	–0.219	2.587	150.7	163.5	8.9	25.5	67.9
	44	3–Picolinium	B3LYP/ 6–311++G(d,p)	132.21	156.3	–0.223	2.582	176.6	178.8	17.9	23.9	53.9
			B3LYP/ 6–311++G(d,p) with GD3	131.95	161.4	–0.217	2.572	173.2	177.1	8.0	23.3	51.0
			M062X/ 6–311++G(d,p)	139.45	178.5	–0.192	2.543	168.0	173.8	8.8	25.1	66.0
			B3LYP/ aug–cc–pVDZ	128.38	157.8	–0.221	2.585	157.4	170.3	7.8	22.4	60.3
			MP2/ aug–cc–pVDZ	120.09	229.2	–0.200	2.562	147.7	166.0	8.1	24.0	66.5
	47	2,6–Lutidinium	B3LYP/ 6–311++G(d,p)	118.65	128.7	–0.270	2.650	173.2	177.2	16.6	22.1	60.5
			B3LYP/ 6–311++G(d,p) with GD3	117.41	140.3	–0.254	2.621	165.2	175.0	7.4	22.1	57.5
			M062X/ 6–311++G(d,p)	131.33	152.3	–0.237	2.598	165.2	176.4	7.9	23.7	68.2
			B3LYP/ aug–cc–pVDZ	115.31	129.6	–0.269	2.648	175.2	178.7	6.8	20.2	50.7
			MP2/ aug–cc–pVDZ	104.72	204.1	–0.218	2.586	144.6	173.0	8.1	24.1	68.4
CH	**60**	Fluoroacetylene	B3LYP/ 6–311++G(d,p)	20.75	44.2	–0.467	3.082	148.4	176.8	4.1	4.2	10.7
			B3LYP/ 6–311++G(d,p) with GD3	17.82	42.7	–0.485	3.119	114.6	159.7	3.4	6.2	16.2
			M062X/ 6–311++G(d,p)	24.64	49.7	–0.452	3.055	146.2	175.1	3.5	5.2	12.3
			B3LYP/ aug–cc–pVDZ	19.83	41.6	–0.462	3.088	143.1	179.7	3.2	4.9	10.2
			MP2/ aug–cc–pVDZ	12.45	43.8	–0.468	3.111	103.0	163.2	3.6	8.2	19.4
	61	Hydrogen cyanide	B3LYP/ 6–311++G(d,p)	39.11	65.2	–0.386	2.944	156.5	177.3	6.3	6.9	17.6
			B3LYP/ 6–311++G(d,p) with GD3	12.54	68.5	–0.378	2.930	145.4	174.9	4.2	7.1	18.0
			M062X/ 6–311++G(d,p)	42.70	68.7	–0.384	2.938	155.0	176.0	3.9	7.7	18.7

			B3LYP/ aug–cc–pVDZ	37.79	61.4	–0.380	2.948	156.3	179.9	3.7	6.6	16.0
			MP2/ aug–cc–pVDZ	35.64	61.9	–0.377	2.952	119.0	171.7	4.1	9.3	27.0
	68	Methane	B3LYP/ 6–311++G(d,p)	2.58	13.6	–0.708	3.598	179.3	179.8	1.6	0.3	3.5
			B3LYP/ 6–311++G(d,p) with GD3	–0.91	15.4	–0.715	3.612	101.6	156.6	1.5	1.2	3.0
			M062X/ 6–311++G(d,p)	4.72	18.7	–0.645	3.470	178.0	179.4	1.7	0.9	4.7
			B3LYP/ aug–cc–pVDZ	2.43	14.9	–0.707	3.608	178.6	179.8	1.2	1.4	2.1
			MP2/ aug–cc–pVDZ	–3.93	17.7	–0.702	3.602	95.9	164.7	1.4	2.6	3.8

[a] – S. Grimme, J. Antony, S. Ehrlich and H. Krieg, *J. Chem. Phys.*, 2010, **132**, 154104.

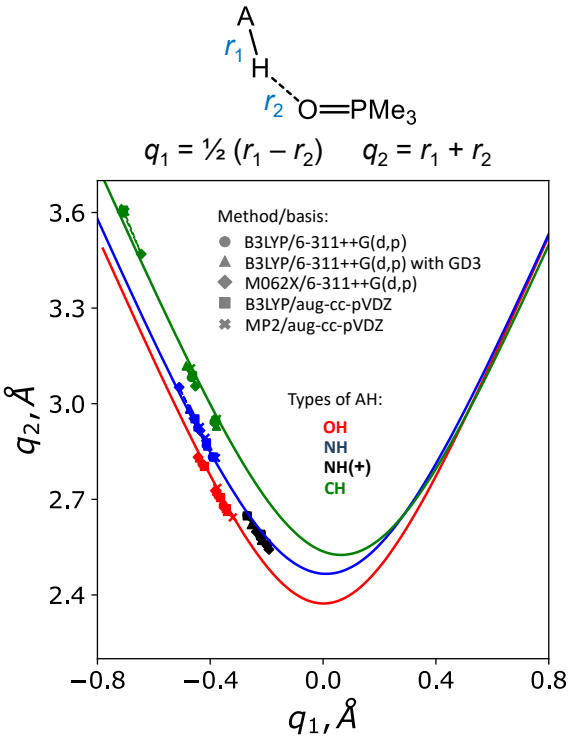

Figure S11. Calculations at various levels of theory and using various basis sets: correlations between q_2 and q_1 natural coordinates of hydrogen bond for selected set of studied complexes (see **Table S1**). The solid lines correspond to **Eqs. 1–3**. The set of points related to result of calculations for the same complex are connected by the dashed lines.

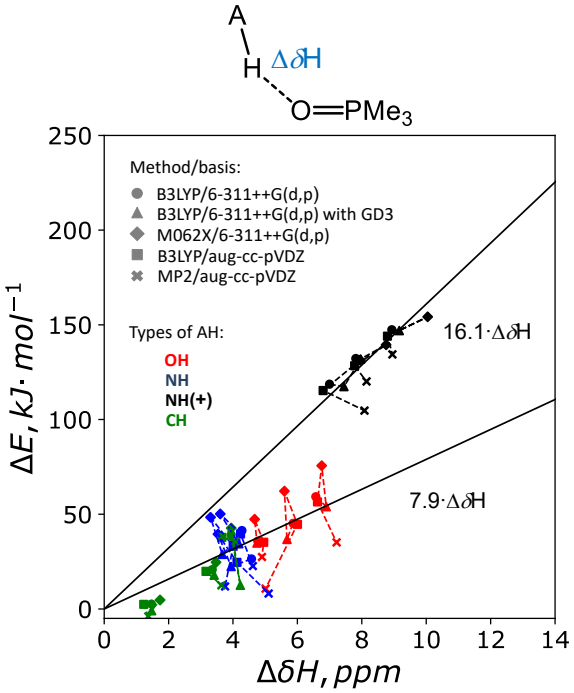

Figure S12. Calculations at various levels of theory and using various basis sets: correlation between ΔE and $\Delta\delta$H for selected set of studied complexes (see **Table S1**). Solid lines correspond to the results of least squares fitting of data points shown in Figure S7. The correlatioin between ΔE and $\Delta\delta$H is different for complexes with cationic and neutral AH molecules. The set of points related to result of calculations for the same complex are connected by the dashed lines.

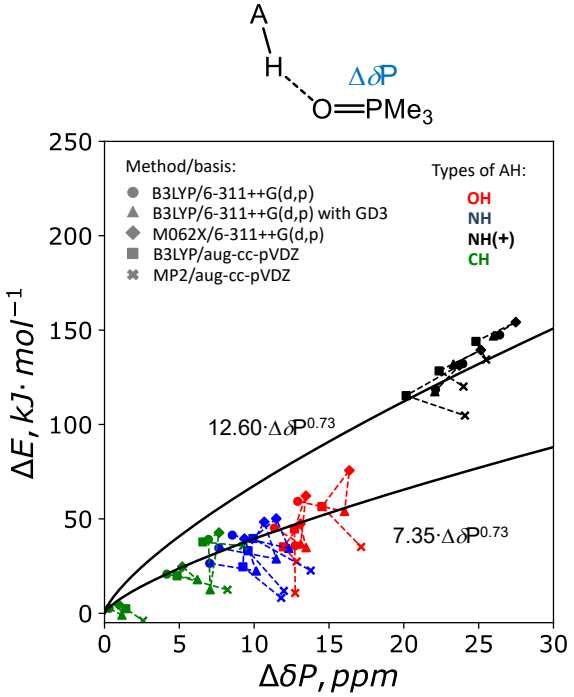

Figure S13. Calculations at various levels of theory and using various basis sets: correlation between ΔE and $\Delta\delta$P for selected set of studied complexes (see **Table S1**). Solid lines correspond to the results of least squares fitting of data points shown in Figure S8. The set of points related to result of calculations for the same complex are connected by the dashed lines. The correlation is different for complexes with cationic and neutral AH molecules.

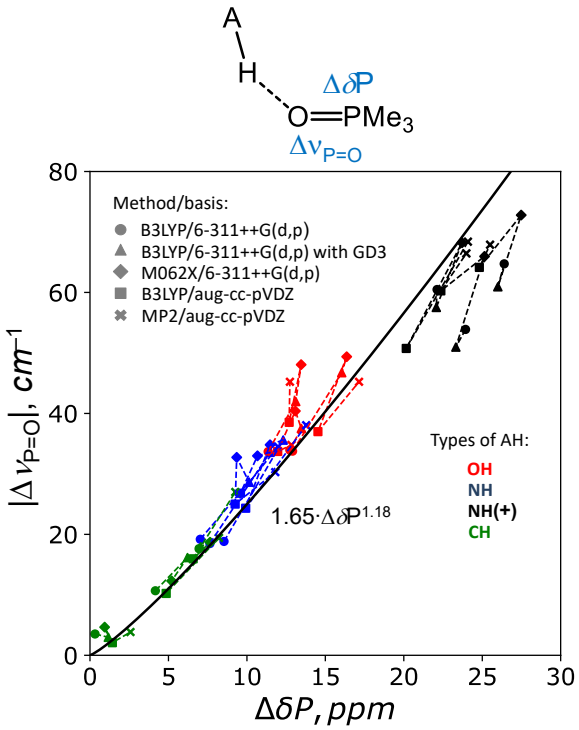

Figure S14. Calculations at various levels of theory and using various basis sets: correlation between $|\Delta \nu_{P=O}|$ and $\Delta\delta$P for selected set of studied complexes (see **Table S1**). The solid line corresponds to the results of least squares fitting of data points shown in Figure S9. The set of points related to result of calculations for the same complex are connected by the dashed lines. The correlation is the same for complexes with cationic and neutral AH molecules.

Table S2. Additional parameters for complexes **1**–**70** in aprotic medium (chloroform): electron density ρ in atomic unit ($|e|\cdot Bohr^{-3}$), Laplacian of electron density $\Delta\rho$ in Hartree. The last column contains references to the literature value of pK_a.

Type of proton donor	No.	Proton donor molecule	ρ	$\Delta\rho$	References to p*K*a
OH	**1**	Water	0.0360	0.1286	T. Silverstein and S. Heller, *J. Chem. Educ.*, **2017**, 94, 690–695.
	2	Methanol	0.0365	0.1306	P. Ballinger and F. Long, *J. Am. Chem. Soc.*, **1960**, 82, 795–798.
	3	Fluoromethanol	0.0481	0.1522	–
	4	Difluoromethanol	0.0602	0.1617	–
	5	Trifluoromethanol	0.0775	0.1672	–
	6	Chloromethanol	0.0536	0.1595	–
	7	Dichloromethanol	0.0694	0.1687	–
	8	Ethanol	0.0353	0.1281	D. DeTar, *J. Am. Chem. Soc.*, **1982**, 104, 7205–7212
	9	2,2,2-Trifluoroethanol	0.0459	0.1493	J. Suh, D. Koh and C. Min, *J. Org. Chem.*, **1988**, 53, 1147–1153
	10	Formic acid	0.0629	0.1603	M. Kim, C. Kim, H. Lee and K. Kim, *J. Chem. Soc. Faraday Trans.*, **1996**, 92, 4951–4956
	11	Acetic acid	0.0579	0.1566	D. Barrón, S. Butí, M. Ruiz and J. Barbosa, *Phys. Chem. Chem. Phys.*, **1999**, 1, 295–298
	12	Chloroacetic acid	0.0687	0.1633	B. Chawla and S. Mehta, *J. Phys. Chem.*, **1984**, 88, 2650–2655
	13	Dichloroacetic acid	0.0759	0.1631	B. Chawla and S. Mehta, *J. Phys. Chem.*, **1984**, 88, 2650–2655
	14	Trichloroacetic acid	0.0830	0.1601	–
	15	Trifluoroacetic acid	0.0856	0.1579	Z. Pawelka and M. Haulait-Pirson, *J. Phys. Chem.*, **1981**, 85, 1052–1057
	16	Benzoic acid	0.0602	0.1583	N. McHedlov-Petrossyan and R. Mayorga, *J. Chem. Soc. Faraday Trans.*, **1992**, 88, 3025–3032
	17	Pentafluorobenzoic acid	0.0734	0.1635	N. McHedlov-Petrossyan and R. Mayorga, *J. Chem. Soc. Faraday Trans.*, **1992**, 88, 3025–3032
	18	Methanesulfonic acid	0.0852	0.1555	J. Guthrie, *Can. J. Chem.*, **1978**, 56, 2342–2354
	19	Benzenesulfonic acid	0.0896	0.1513	J. Guthrie, *Can. J. Chem.*, **1978**, 56, 2342–2354
	20	p-Toluenesulfonic acid	0.0911	0.1484	–
	21	Phenylphosphonic acid	0.0672	0.1616	H. Jaffé, L. Freedman and G. Doak, *J. Am. Chem. Soc.*, **1953**, 75, 2209–2211
	22	Phenol	0.0459	0.1483	G. Bouchard, P. Carrupt, B. Testa, V. Gobry and H. Girault, *Chem. Eur. J*, **2002**, 8, 3478–3484
	23	2-Nitrophenol	0.0560	0.1599	W. Mock and L. Morsch, *Tetrahedron*, **2001**, 57, 2957–2964
	24	3-Nitrophenol	0.0515	0.1588	J. Llor, *J. Solution Chem.*, **1999**, 28, 1–20
	25	4-Nitrophenol	0.0550	0.1612	W. Mock and L. Morsch, *Tetrahedron*, **2001**, 57, 2957–2964
NH	**26**	Ammonia	0.0195	0.0731	–
	27	Dimethylamine	0.0202	0.0768	–
	28	Aziridine	0.0229	0.0861	S. Searles, M. Tamres, F. Block and L. Quarterman, *J. Am. Chem. Soc.*, **1956**, 78, 4917–4920
	29	Azetidine	0.0199	0.0740	S. Searles, M. Tamres, F. Block and L. Quarterman, *J. Am. Chem. Soc.*, **1956**, 78, 4917–4920
	30	Pyrrolidine	0.0196	0.0719	S. Searles, M. Tamres, F. Block and L. Quarterman, *J. Am. Chem. Soc.*, **1956**, 78, 4917–4920
	31	Piperidine	0.0196	0.0734	S. Searles, M. Tamres, F. Block and L. Quarterman, *J. Am. Chem. Soc.*, **1956**, 78, 4917–4920
	32	Piperazine	0.0194	0.0723	C. Bernasconi, J. Moreira, L. Huang and K. Kittredge, *J. Am. Chem. Soc.*, **1999**, 121, 1674–1680
	33	2-Pyrrolidone	0.0312	0.1095	–
	34	Pyrrole	0.0326	0.1232	A. Gervasini and A. Auroux, *J. Phys. Chem.*, **1993**, 97, 2628–2639
	35	Imidazole	0.0366	0.1349	B. Barszcz, M. Gabryszewski, J. Kulig and B. Lenarcik, *J. Chem. Soc. Dalt. Trans.*, **1986**, 2025–2028
	36	Pyrazole	0.0377	0.1315	B. Barszcz, M. Gabryszewski, J. Kulig and B. Lenarcik, *J. Chem. Soc. Dalt. Trans.*, **1986**, 2025–2028
	37	1,4-Dihydropyrazine	0.0277	0.1080	–
NH^+	**38**	Ammonium	0.0727	0.1577	Y. Yan, E. Zeitler, J. Gu, Y. Hu and A. Bocarsly, *J. Am. Chem. Soc.*, **2013**, 135, 14020–14023
	39	Dimethylammonium	0.0595	0.1649	–
	40	Trimethylammonium	0.0575	0.1659	–
	41	Imidazolium	0.0629	0.1621	S. Datta and A. Grzybowski, *J. Chem. Soc. B Phys. Org.*, **1966**, 136–140
	42	Pyridinium	0.0650	0.1668	A. Isao, U. Kikujiro and K. Hirondo, *Bull. Chem. Soc. Jpn.*, **1982**, 55, 713–716
	43	2-Picolinium	0.0589	0.1651	–
	44	3-Picolinium	0.0630	0.1669	–
	45	4-Picolinium	0.0621	0.1653	–
	46	3,5-Lutidinium	0.0621	0.1659	–
	47	2,6-Lutidinium	0.0540	0.1603	–
	48	2,4,6-Collidinium	0.0528	0.1604	–
	49	2-(Dimethylamino)pyridinium	0.0465	0.1510	–
	50	3-(Dimethylamino)pyridinium	0.0594	0.1642	–
	51	4-(Dimethylamino)pyridinium	0.0532	0.1580	C. Heo and J. Bunting, *J. Org. Chem.*, **1992**, 57, 3570–3578
	52	3,5-(Dimethylamino)pyridinium	0.0560	0.1620	–
	53	3,4,5-(Trimethoxy)pyridinium	0.0576	0.1677	–
	54	3,4,5-Trifluoropyridinium	0.0839	0.1653	–
	55	3,4,5-Trichloropyridinium	0.0805	0.1675	–
	56	3,5-Aminopyridinium	0.0598	0.1641	–
CH	**57**	Trifluoroethylene	0.0202	0.0803	–
	58	Trichloroethylene	0.0208	0.0814	–
	59	Acetylene	0.0214	0.0862	–
	60	Fluoroacetylene	0.0217	0.0896	–
	61	Hydrogen cyanide	0.0344	0.1301	K. Ang, *J. Chem. Soc.*, **1959**, 3822–3825
	62	Trinitromethane	0.0440	0.1469	–
	63	1,1-Dinitroethane	0.0271	0.1034	J. Belew and L. Hepler, *J. Am. Chem. Soc.*, **1956**, 78, 4005–4007
	64	2-Nitropropane	0.0145	0.0473	H. Gilbert, *J. Am. Chem. Soc.*, **1980**, 102, 7059–7065
	65	Trichloromethane	0.0269	0.1046	K. Klabunde and D. Burton, *J. Am. Chem. Soc.*, **1972**, 94, 5985–5990
	66	Dichloromethane	0.0210	0.0797	–
	67	Chloromethane	0.0145	0.0517	–
	68	Methane	0.0047	0.0154	–
	69	Trifluoromethane	0.0233	0.0942	–
	70	Tribromomethane	0.0262	0.1015	K. Klabunde and D. Burton, *J. Am. Chem. Soc.*, **1972**, 94, 5985–5990

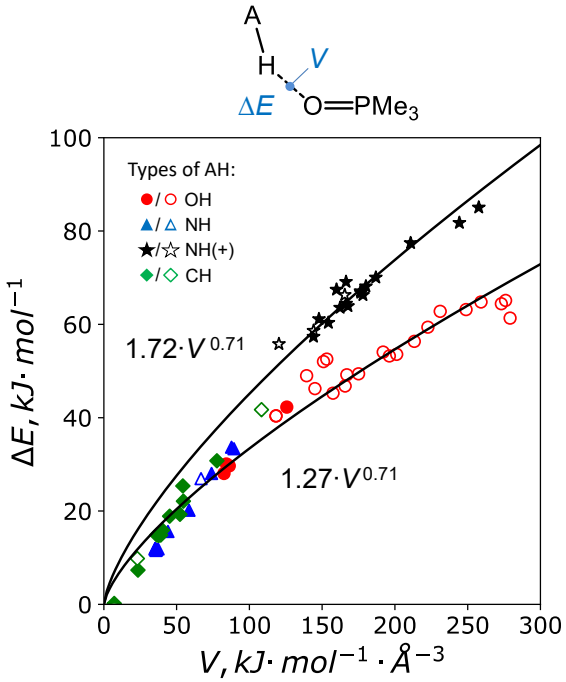

Figure S15. The complexes of Me_3PO in aprotic medium: correlation between ΔE and V. Solid lines correspond to the result of least squares fitting of data points by the functions $\Delta E = k \cdot V^{0.71}$. The coefficient k is different for complexes with cationic and neutral AH molecules. The power equal to 0.71 was fixed due to strong correlation $G(V)$ shown in Figure 11 and linear correlation $\Delta E(G)$ shown in Figure 10.

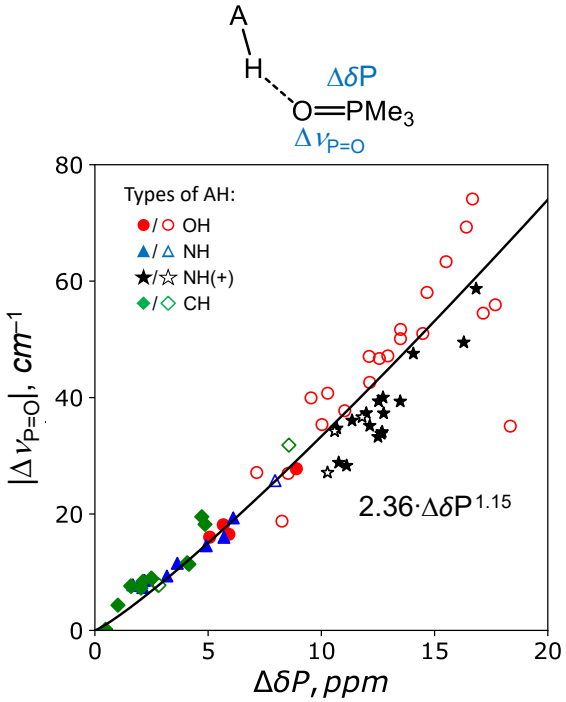

Figure S16. The complexes of Me_3PO in aprotic medium: correlation between $|\Delta \nu_{P=O}|$ and $\Delta\delta P$. Solid line corresponds to the correlation function obtained as the results of least squares fitting of correlations $G(|\Delta \nu_{P=O}|)$ shown in Figure 12 and $G(\Delta\delta P)$ shown in Figure 14. Correlation between $|\Delta \nu_{P=O}|$ and $\Delta\delta P$ is the same for both complexes with cationic and neutral AH molecules.

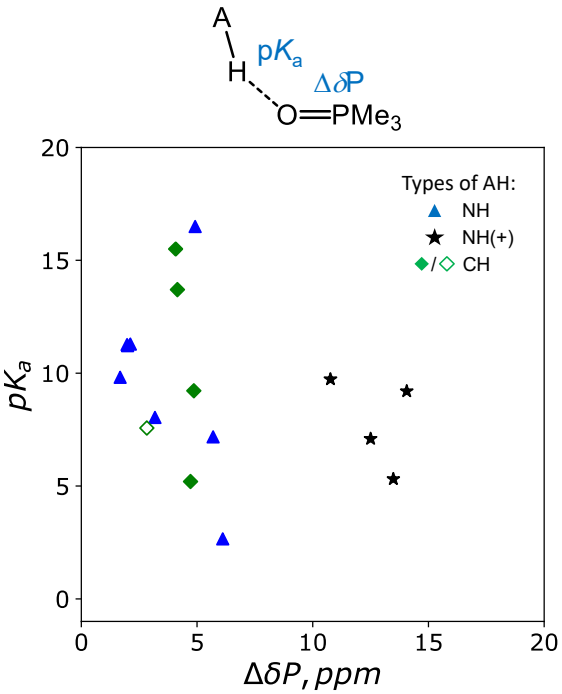

Figure S17. The complexes of Me_3PO in aprotic medium: $\Delta\delta$P and pK_a for NH, NH^+ and CH proton donors. The values of pK_a are taken from the literature (see **Table S2**).

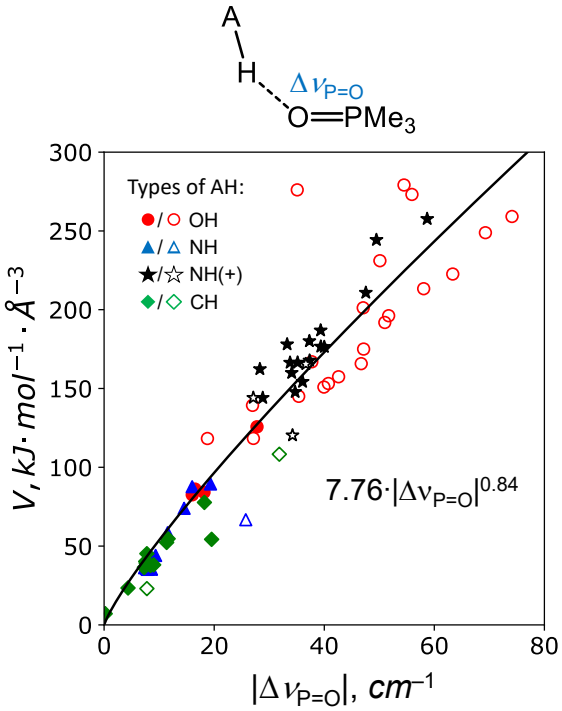

Figure S18. The complexes of Me_3PO in aprotic medium: correlation between V and $|\Delta\nu_{P=O}|$. Solid line corresponds to the result of least squares fitting of data points by the power function. The correlation $V(|\Delta\nu_{P=O}|)$ is the same for both complexes with neutral and cationic molecules.

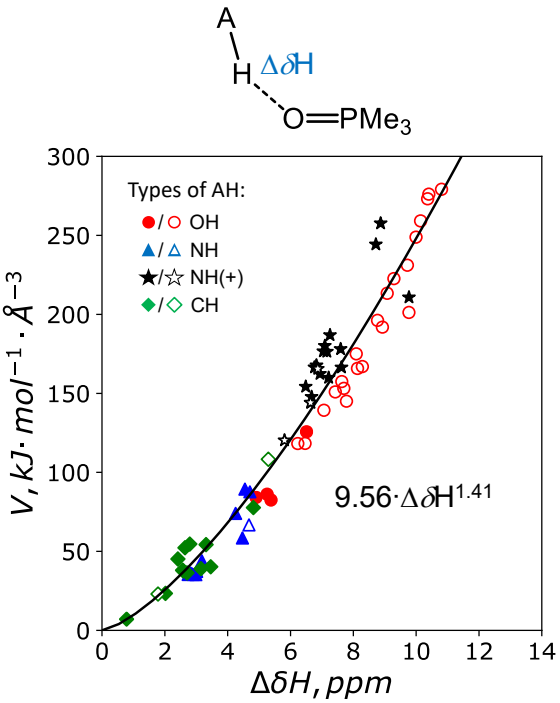

Figure S19. The complexes of Me_3PO in aprotic medium: correlation between V and $\Delta\delta$H. Solid line corresponds to the correlation function obtained as the results of least squares fitting of $G(\Delta\delta H)$ shown in Figure 13 and $G(V)$ shown in Figure 11. The correlation $V(\Delta\delta H)$ is the same for both complexes with neutral and cationic molecules.

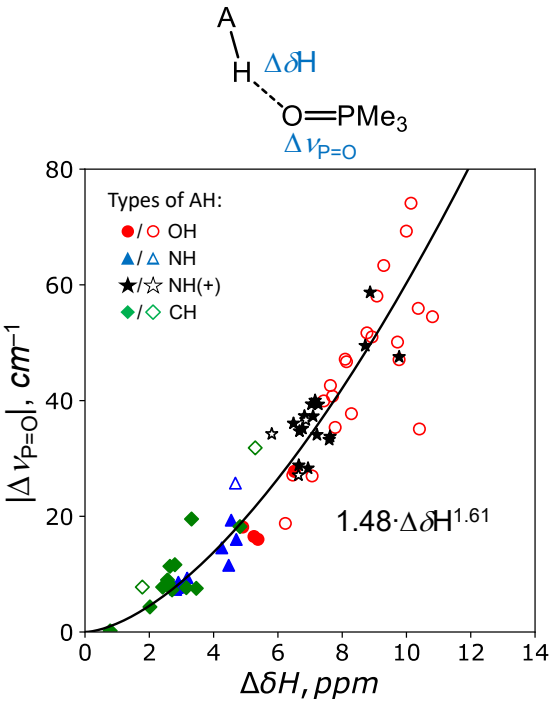

Figure S20. The complexes of Me_3PO in aprotic medium: correlation between $|\Delta\nu_{P=O}|$ and $\Delta\delta$H. Solid line corresponds to the correlation function obtained as the results of least squares fitting of correlations $G(|\Delta\nu_{P=O}|)$ shown in Figure 12 and $G(\Delta\delta H)$ shown in Figure 13. Correlation between $|\Delta\nu_{P=O}|$ and $\Delta\delta$H is the same for both complexes with cationic and neutral AH molecules.

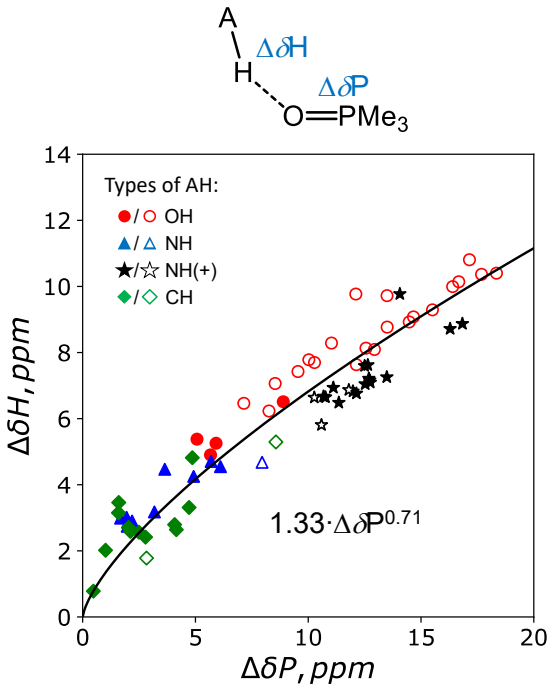

Figure S21. The complexes of Me_3PO in aprotic medium: correlation between $\Delta\delta$H and $\Delta\delta$P. Solid line corresponds to the correlation function obtained as the results of least squares fitting of correlations $G(\Delta\delta H)$ shown in Figure 13 and $G(\Delta\delta P)$ shown in Figure 14. Correlation between $\Delta\delta$P and $\Delta\delta$H is the same for both complexes with cationic and neutral AH molecules